

# Bearing faults identification and resonant band demodulation based on wavelet de-noising methods and envelope analysis

Ahmed M Abdelrhman<sup>1,\*</sup>, Yong Sei Kien<sup>1</sup>, M Salman Leong<sup>2</sup>, Lim Meng Hee<sup>3</sup>,  
Salah M Ali Al-Obaidi<sup>2</sup>

<sup>1</sup>Curtin University Malaysia, CDT 250 98009, Miri, Sarawak, Malaysia

<sup>2</sup>Institute of Noise and Vibration, University Technology Malaysia, Malaysia

<sup>3</sup>UTM Razak School of Engineering and Advanced Technology, Malaysia

E-mail: [ahmed.mohammed@curtin.edu.my](mailto:ahmed.mohammed@curtin.edu.my)

**Abstract.** The vibration signals produced by rotating machinery contain useful information for condition monitoring and fault diagnosis. Fault severities assessment is a challenging task. Wavelet Transform (WT) as a multivariate analysis tool is able to compromise between the time and frequency information in the signals and served as a de-noising method. The CWT scaling function gives different resolutions to the discretely signals such as very fine resolution at lower scale but coarser resolution at a higher scale. However, the computational cost increased as it needs to produce different signal resolutions. DWT has better low computation cost as the dilation function allowed the signals to be decomposed through a tree of low and high pass filters and no further analysing the high-frequency components. In this paper, a method for bearing faults identification is presented by combing Continuous Wavelet Transform (CWT) and Discrete Wavelet Transform (DWT) with envelope analysis for bearing fault diagnosis. The experimental data was sampled by Case Western Reserve University. The analysis result showed that the proposed method is effective in bearing faults detection, identify the exact fault's location and severity assessment especially for the inner race and outer race faults.

## 1. Introduction

Rolling element bearings are classified as the most important and most common component in rotating machinery [1]. It is reported that failure in machinery is commonly caused by the faulty bearings. Figures show that faults in bearing causes approximately 45% in machine breakdown and 40% of problems in rotating machinery [2]. In today's industries, the faults diagnosis of the rotating machinery is becoming a challenging problem and it has gained the attention from worldwide as it is realized that the early faults detection is essential for proper maintenance and prevent catastrophic failures. Therefore, research on the fault diagnosis and fault detection are still ongoing and they are gaining wide attention to prevent sudden failures.

The vibration signals and acoustics emission (AE) is the most commonly used techniques in condition monitoring and diagnosis of rotating machinery. The possibility of machinery failure such as mass unbalance, shaft misalignment, gear failures and bearing defects could be detected using vibration signals of a machine operating either in good or faulty condition [3]. The vibration signals contain rich information and it has been widely used for condition monitoring without interfering the machine operations. So, the vibrations signal are favoured to become the common approach for rotating machinery condition monitoring and fault diagnosis [4].



Vibration signals of the bearing could be classified into stationary and non-stationary signals. In reality, the signal of the bearing is always non-stationary due to the dynamic as the load and speed condition varies over time. The non-stationary signals are somehow treated at stationary signals for short time window method for the ease of computation. The non-stationary signals are complex and associated with a lot of noises. This has caused difficulties in determining the bearing faults by conventional time domain and frequency domain methods which assume that the signal is strictly periodic for analysis [5]. The time-domain features are good for fault detection but weaker fault isolation as compared to the frequency-domain features [6]. The needs for effective detection of the non-stationary signal is getting more demanding to prevent the sudden machine failures. Therefore, various signal processing techniques have been developed to overcome the problem.

Time domain features represent the vibration signal in the function of time where the amplitude of the waveform is plotted over time. It represents the proximity, velocity, and acceleration of the vibration signal. It is favourable to be used for fault diagnosis due to the advantages of a minimum data loss prior the inspection [7]. The time domain features mainly focus on the statistical characteristic of the vibration signal such as the peak level, standard deviation, skewness etc. The disadvantage of the time domain is the possibility of using too much data for easy and clear fault diagnosis [8].

In frequency domain analysis, the Fast Fourier Transform (FFT) transform the signals very quickly and gives the same result as the slower Discrete Fourier Transform (DFT) [9]. The limitation of this approach is that it is not able to analyse the non-stationary signals [10]. The Short Time Fourier Transform is then developed to overcome the limitation of FFT. The STFT is only applicable to analyse the quasi-stationary signals that are stationary at the short time window scale but not applicable to analyse highly transient phenomena in signals, such as impulse [11]. SFTF is inherently not able to determine time-dependent variation in the structure of the window at various scale [12]. For time-frequency analysis, The Empirical Mode Decomposition (EMD) is gaining the attention of the researchers due to its ability of decomposing non-linear or non-stationary signal into a series of zero-mean amplitude-modulation frequency-modulation (AM-FM) [13]. However, some researchers stated that The EDM is mainly to qualitative diagnosis that focusing on the type of severity of the faults but not the quantitative aspect such as the defect size [14]. Wavelet Transform (WT) has been introduced as an effective tool for machinery fault diagnosis. Wavelet itself is not a new theory as it is made up by combining many existing, well-known and independent signal processing techniques such as sub-band coding, quadrature mirror filter, etc. Due to the wide application, wavelet theory is becoming more active in the research fields as it is capable of further improvement in both the mathematical understanding and the wide range of applications in science and engineering [15-17]. The major merits of wavelet are that it is suitable for wideband signals that are not periodic and may contain both sinusoidal and impulse components. It has the ability to analyse the singularities and irregular signal structure and provides an excellent frequency resolution of the spectra, the variance of estimated power spectra and complexity [18].

In this paper, a method for bearing faults detection is formulated by combing CWT and DWT with envelope analysis. The WT was employed as a de-noising process to filter out the other frequencies than the resonance frequency band. This served as a standard reference to centre the band-pass filter for envelope analysis. So, by knowing the exact location of filtering, this would be a better approach to predict the fault severities using the frequency analysis.

## **2. Background Theory**

An antifriction bearing consists of different components such as outer race, inner race, rolling element, and the cage was considered in this study. The inner race is strongly mounted to the shaft to rotate in the shaft speed with the outer race stay stationary during operation while the rolling elements and cage are rotating or spinning at their own speed. In fault diagnosis, the rolling elements play a big role in the frequency recognition where unique frequency will be generated by the faulty component when the rolling elements rolled pass through the fault location. The derivation of the equations measuring the frequency of defective component is based on the relationship between the rotating elements of a bearing

and the relative rotating speed. A defective bearing in a running machine can generate at least five frequencies [19], these frequencies are as following:

a) FTF - Fundamental Train Frequency. It is also known as the frequency of the defected cage:

$$f(\text{Hz}) = \frac{1}{2}s \left[ \frac{BD}{PD} \cos\beta \right] \quad (1)$$

b) BPFI - Bass Pass Frequency of the Inner Race. This is the frequency that produced during the rolling elements roll across the defected inner race:

$$f(\text{Hz}) = \frac{n}{2}s \left[ 1 + \frac{BD}{PD} \cos\beta \right] \quad (2)$$

c) BPFO – Bass Pass Frequency of Outer Race. This is the frequency that produced during the rolling elements roll across the defected outer race.

$$f(\text{Hz}) = \frac{n}{2}s \left[ 1 - \frac{BD}{PD} \cos\beta \right] \quad (3)$$

d) BSF – Ball Spin Frequency. This is the circular frequency of each rolling elements.

$$f(\text{Hz}) = \frac{PD}{2 \times BD} s \left[ 1 - \left( \frac{BD}{PD} \cos\beta \right)^2 \right] \quad (4)$$

e) Rolling Element Defect Frequency. This frequency is twice the BSF.

$$f(\text{Hz}) = \frac{PD}{BD} s \left[ 1 - \left( \frac{BD}{PD} \cos\beta \right)^2 \right] \quad (5)$$

where  $s$  is speed (revolutions per minute),  $n$  is the number of the rolling elements,  $\beta$  is contact angle (degrees),  $BD$  is ball or roller diameter and  $PD$  is Pitch diameter. In this paper, the contact angle is zero degree.

### 3. Signals Analysis Techniques

#### 3.1. Continuous Wavelet Transform

Wavelet Transform is a revolution from the Fast Fourier Transform (FFT). The multi-resolution of time-frequency analysis has resolved the limitation of FFT. Consider a function  $\psi$  having complex-valued satisfying the following conditions:

$$\int_{-\infty}^{\infty} |\psi(t)|^2 dt < \infty \quad (6)$$

$$C_{\psi} = 2\pi \int_{-\infty}^{\infty} \frac{|\Psi(\omega)|^2}{|\omega|} d\omega < \infty \quad (7)$$

where  $\Psi$  is defined as the Fourier transform of  $\psi$ . The first condition represents the finite energy of the function  $\psi$ . The second condition is the admissibility condition, it represents that if  $\Psi(\omega)$  is smooth then the  $\Psi(0) = 0$ . The function  $\psi$  is the mother wavelet. The theory could be explained as the following: Let  $f(x)$  be the signal and the CWT of  $f(x)$  is then defined as:

$$W_f(a, b) = \int_{-\infty}^{+\infty} f(x) \psi_{ab}^*(x) dx \quad (8)$$

The (\*) represent the complex conjugate

$$\psi_{ab}(x) = \frac{1}{\sqrt{|a|}} \psi\left(\frac{x-b}{a}\right) \quad a, b \in R, a \neq 0 \quad (9)$$

The admissibility condition is described as

$$C_\psi = \int_0^\infty \frac{|\psi(\omega)|^2}{\omega} d\omega < \infty \quad (10)$$

And it yields to:

$$\int_{-\infty}^{\infty} \psi(x) dx = 0 \quad (11)$$

The  $\psi(\omega)$  is Fourier transform of the  $\psi(x)$ . The admissibility condition describes that the Fourier transform of  $\psi(x)$  will be cancelled off at zero frequency. From this, it is clearly to present that  $\psi$  is described as a wave or the mother wavelet. It has two characteristic parameters which is (a) dilation and (b) translation which varies continuously. The function of the translation is to control the position of wavelet in time. The high-frequency information could be obtained by narrowing down the wavelet while the dilated wavelet accesses the low-frequency information. This could be said that the parameter  $a$  varies with different frequencies [20].

### 3.2. Discrete Wavelet Transform

DWT is derived from the discretization of CWT to reduce the computation cost when operating at every scale. It is opposite to the CWT, the scaling parameter  $a$  and the time localization parameter  $b$  are defined as

$$a = 2^j, j \in Z \quad (12)$$

$$b = k2^j, j, k \in Z \quad (13)$$

where  $Z = 0, \pm 1, \pm 2, \dots$ . The discretization scaling and time parameter is the property of DWT such that:

$$DWT_{j,k} = \int_{-\infty}^{\infty} x(t) \psi^*\left(\frac{t-k}{2^j}\right) dt \quad (14)$$

In order for the discretization to occur, the CWT becomes DWT function, the scaling function is given by:

$$\psi_{jk} = \int_{-\infty}^{\infty} x(t) \psi^*\left(\frac{t-k}{2^j}\right) dt \quad (15)$$

$$\phi_{jk} = \int_{-\infty}^{\infty} x(t) \phi^*\left(\frac{t-k}{2^j}\right) dt \quad (16)$$

Then, the wavelet coefficient of a signal  $x(t)$  can be defined as

$$a_{2^j k} = \int_{-\infty}^{\infty} x(t) \psi_{j,k} dt \quad (17)$$

$$a_{2^j k} = \int_{-\infty}^{\infty} x(t) \phi_{j,k} dt \quad (18)$$

Consequently, the discretization property can decompose the signal into a hierarchical structure with wavelet details and approximations at various scale [21].

### 3.3. Envelope Analysis

The envelope analysis demodulates the amplitude modulating (AM) signal to extract the signal signature using three steps. Firstly, the signals are filtered using the band-pass filter centered at the resonant frequency band. The filtering effects will eliminate the unwanted side band's high amplitude contents and suppress the high-frequency noise. Therefore, a signal with a good signal-to-noise ratio (SNR) can be obtained.

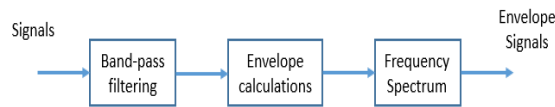


**Figure 1.** The signals flow in envelope analysis

The Hilbert Transformation (HT) is acted as the processor that perform the calculation or the envelope signal. Consider the input signal is FFT, the HT process signal and create analytical signal using the following algorithm:

$$Signal = X_{in} = fft(x_{in}) \quad (19)$$

$$X_a(n) = \begin{cases} X_{in}(n), & \text{if } n = \frac{N}{2} \\ 2 \times X_{in}(n), & \text{if } 0 < n \leq \frac{N}{2} \\ 0, & \text{if } \frac{N}{2} < n < N \end{cases} \quad (20)$$

$$x_a = ifft(X_a) \quad (21)$$

The created signal is a complex signal in nature. The real part is the original signal and the imaginary part is the Hilbert transform of the original signal. The envelope signal is computed using

$$x_{env} = \sqrt{x_a \times conj(x_a)} \quad (22)$$

The signal is then converted to the frequency spectrum using the next equation where the  $\bar{x}_{env}$  is the mean value of the envelope which is first substrate to remove the offset component. The Hanning window is employed to reduce the tendency of spectral leakage which is given by the following [22].

$$x_{env} = |fft((x_{env} - \bar{x}_{env}) \times hann(N))| \quad (23)$$

## 4. Data Acquisition

The vibration signals used in this study is obtained from the Case Western Reserve University. The apparatus used consists of 2 horsepower motor (left), a torque transducer/encoder (centre), a dynamometer (right), and control electronics (not shown) in the following figures. The vibration signals data sets for the different type of bearing condition were obtained, namely, inner race, outer race, rolling element fault and healthy bearing. The test bearings support the motor shaft so that the bearings can rotate as the motor rotate. Single point faults were introduced to the test bearing using the electro-discharge machining with fault diameter of 7 mils, 14 mils, 21 mils, 28 mils, and 40 mils (1mil=0.001 inches).

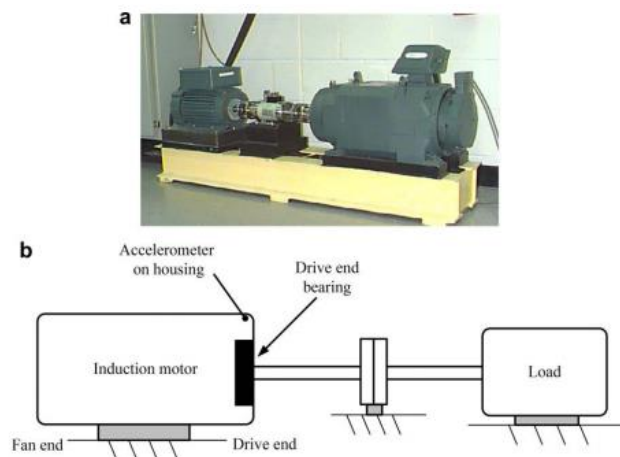


**Figure 2.** (a) Bearing test rig; (b) Its schematic representation

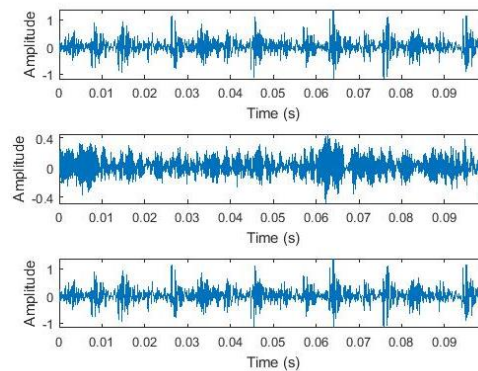


**Figure 3.** Time-wave of bearing raw signals: (upper) healthy (middle) inner race fault (bottom) outer race fault

The accelerometers were attached to the different positions of the housing with magnetic based to collect the vibration data. The positions include the 12 o'clock position at both the drive end and fan end of the motor housing where one of it is attached to the motor supporting base plate for some experiment. The vibration signals were collected using a 16 channel DAT recorder and were post processed using the MATLAB. The motor runs at different speeds typically from 1730 -1797 rpm and the bearing was run under different load condition 0, 1, 2, 3, 4 motor horsepower. The data were sampled at 12 kHz sampling frequency. To evaluate the purpose of this paper, the signals with zero loading, 0 horsepower obtained at the drive end location were used. The bearing was test run at 1797 rpm and the data used contained 120,000 data points with 10-second time span. The model of the bearing is 6205-2RS JEM SKF, deep groove ball bearing and the defect frequencies are summarized as the following [23].

**Table 1.** 2RS JEM SKF, deep groove ball bearing defect frequencies

Ball Passing Frequency	multiple of running speed in Hz
	Defect Frequency (Hz)
BPFI	5.4152
BPFO	3.5848
FTF	0.39828
$2 \times$ BPF	4.7135

## 5. Results and Discussion

### 5.1. Continuous Wavelet Transform and Envelope Analysis

In this study, Morlet wavelet mother function is employed for all the continuous wavelet transform process to correlate the bearing signals impulse and remove the noise present in the signals. In the process of CWT, the entire input signal was ‘dismantled’ and re-arranged according to the energy level content in the wavelet coefficient. The high-frequency components have a finer resolution and the lower have a courser resolution. So, the signal with higher energy content was located at the smaller scale while the signal with lower energy content was located at the higher scale. The energy content of the signal was identified by viewing the amplitude of the signal that corresponded to its scale in the wavelet coefficient. The higher amplitude component in the signal has brighter color at the coefficient map. According to the Figure 4, defective bearings often has lower scale than the normal bearing which is scale 3 and scale 9 respectively which indicated that the detective bearings have higher energy content than the normal bearing. The rolling element rolled pass the defective part created large impulse and produced high frequency during the operation. The defective bearing generated frequency as high as 2.6 kHz to 5.0 kHz which was known as the resonant frequency band of the defective bearing. The CWT was able to eliminate the other frequency components and remain only resonance frequency in the entire signals. As the resonance frequency band was identified, the band-pass filter was centered in such a way that it covered the entire resonance band in the envelope analysis. This is to ensure the band-pass filter could be accurately applied to the resonance band for high-frequency demodulation when assessing the increasing fault severities.

Figure 4(e), (f), (g) and (h) present the frequency spectrum of healthy bearing, inner race, outer race and rolling elements faults. The resonant band was treated as 2.5 kHz – 5 kHz. By centering the band-pass filter on the frequency band of 2.5 kHz – 5 kHz would yield frequency spectrum that reviewed the faulty characteristic frequency of the bearing in envelope analysis. To effectively assess the fault severities of the bearing, the exactly resonant frequency range have to be determined. This could be done using the CWT scale function to de-noising the signal and retain only the resonant band in the entire signal. For inner race fault, it is clearly seen that the peak generated by the characteristic frequency, BPFI, 162.18 Hz is prominent. The frequency spectrum did not show exactly the 162.18 Hz at the characteristic frequency as the bearings were not always in the no slip condition which the theoretical formula assumed that the bearing is in no slip condition. For the outer race fault, all the frequency spectrum showed that the BPFO 107.6Hz is prominent for 0.007” fault size and BPFO for the 0.021” fault size are evidenced but the opposite signals contained more other frequency component compared to the others. The frequency spectrum of rolling element fault contained the characteristic frequency of inner race, outer fault, and rolling element fault. In close inspection to the frequency spectrum of outer race fault, it was observed that the fundamental train frequency, FTF is presented along with second and third harmonics. Other than that, it was also observed that the unit speed and its harmonics are found in the spectrum that was labeled in ‘x’ multiple that indicated residual imbalance, loading, and looseness. There are many other frequencies and their harmonics contained in frequency are mainly due to many other frequency modulations presented in the resonance frequency band. In this analysis, results showed the harmonic of BPFI and BPFO indicated the fault location contained fragment denting or frosting [19]. The amplitude of the characteristic frequency and its harmonic are shown to be increased when the fault size increase.

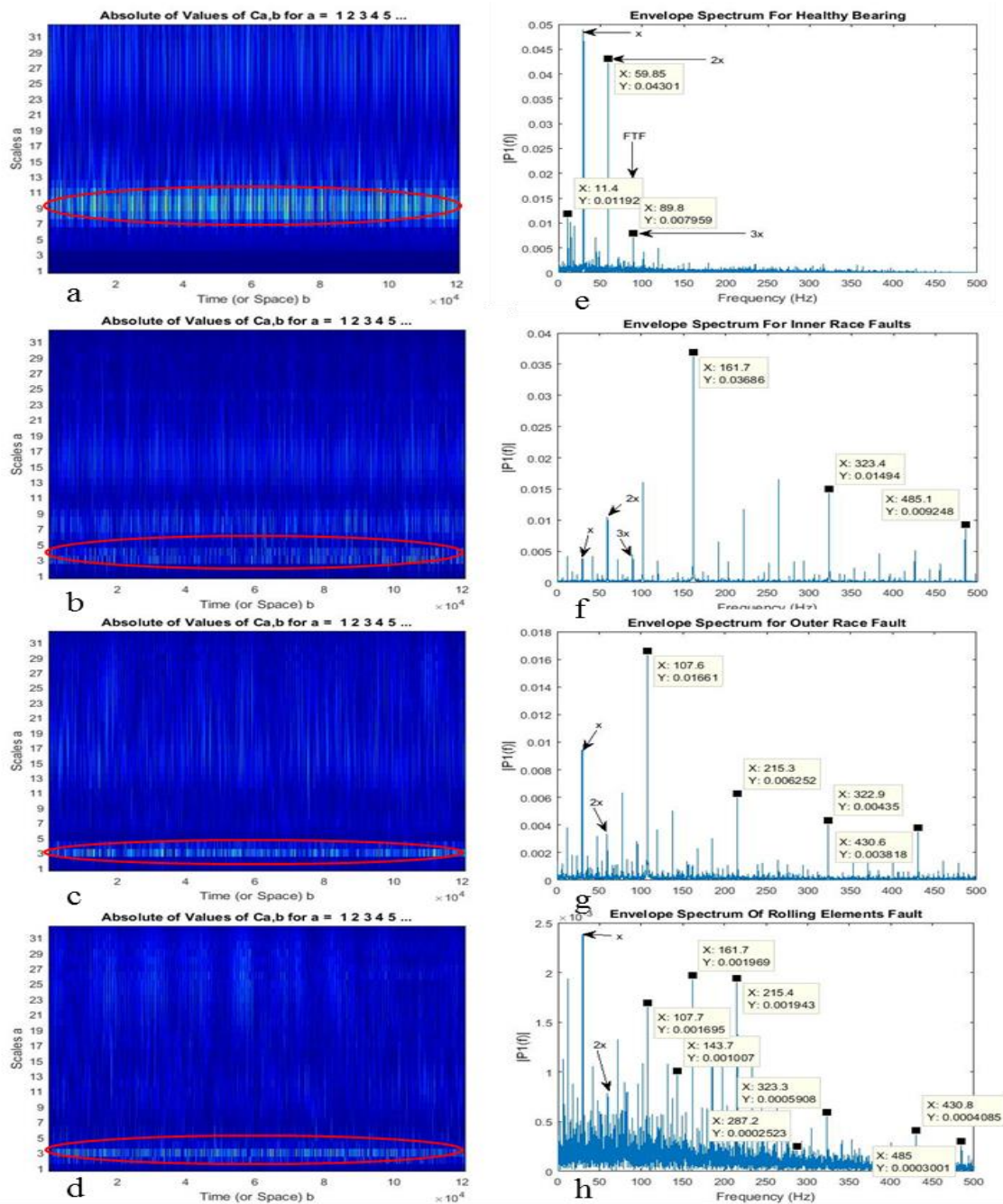


**Figure 4.** Wavelet coefficients map of different bearing faults, (a) healthy (b) inner race (c) outer race (d) Rolling elements; frequency spectrum for (e) healthy (f) inner race fault (g) outer race fault (h) rolling elements fault.

### 5.2. Discrete Wavelet Transform and Envelope Analysis

DWT is another important part of the wavelet transform that could perform very well in de-noising using the built-in high pass and low pass filters. The main function of the DWT is to decompose the signal into smaller frequency band to detect the pattern that is not visible in the signals. On the other hand, DWT also reassembles back the decomposed signal to its original signal without any loss of information. In this section, detection of bearing fault using the signal reconstruction in DWT and envelope analysis

is presented. The mother wavelet employed for this work is 'db4' wavelet. The 'db4' function is similar to the bearing impulse but when compared to the Morlet function, a distinct difference was found between them in the terms of the time and amplitude due to the orthogonality.

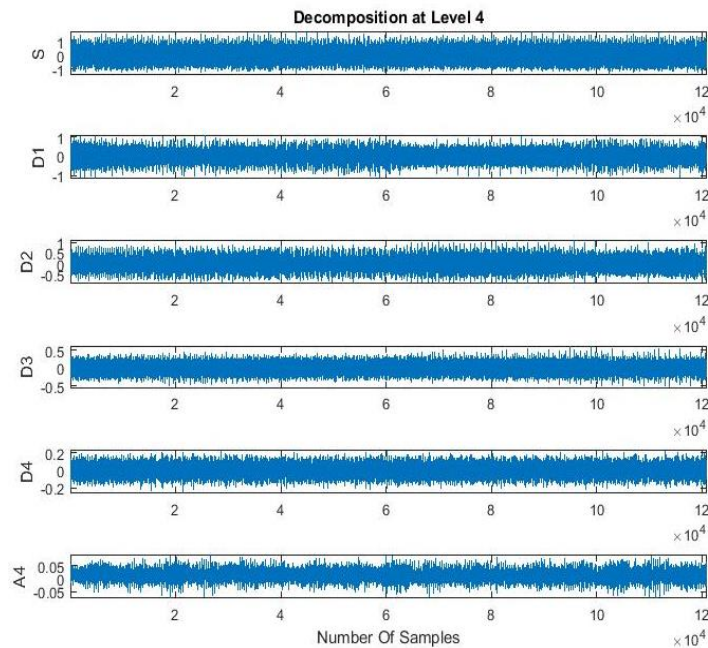
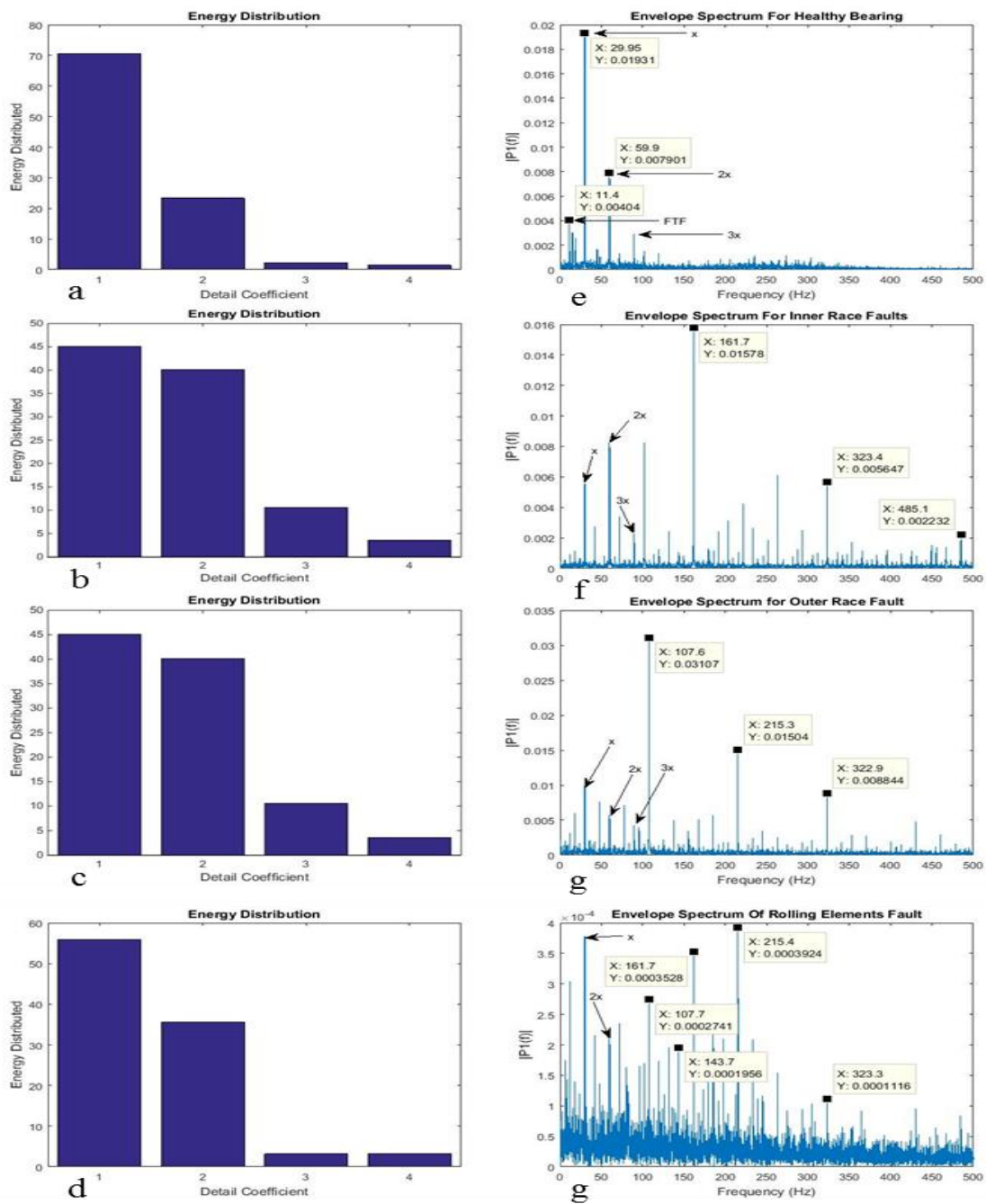


Figure 5: Signal Reconstruction Using DWT

The DWT decomposed the signal into the detail part and approximate part. The detail part of the decomposition contains the energy distribution of the signal which it is the key point for fault diagnosis. The benefit of the signal reconstruction is that the number of the samples are retained after the decomposition so that the frequency resolution can be maintained at the higher decomposition level. Using DWT to search for the high- frequency carrier is generally easier and has less computation time compared to the CWT. DWT processed the signals by decomposing the signals through the high-pass and the low-pass filters in the down-sampling of 2. In a close look into this process, the high-pass filtering process stopped after the higher frequency signals components were identified which only the lower frequency component would be decomposed in the next subsequent low-pass and high-pass filtering.

In this study, all the signals for the different bearing condition are decomposed to four level of decomposition as shown in Figure 5. According to Nyquist, the 12 kHz sampling rate signal would have the frequency halved the sampling rate which is 6 kHz. The frequency bands which reduced half at each decomposition level, are sequentially 3 kHz, 1.5 kHz, 750 Hz and 325 Hz. The faulty frequencies are in the range of 325 Hz. Therefore, further decomposition is not necessarily. The energy distribution in each of the decomposed signals is examined. Then, the frequency band which has the highest distributed energy among the detail part were extracted for envelope analysis. The resonance frequency band retained by the DWT is different from the one in CWT. DWT retained a wider frequency band due to the different wavelet function used. The 'db4' function is similar to the bearing impulse but when compared to the Morlet function, a distinct difference was found between them in the terms of the time and amplitude and resulted in the differences in the frequency spectrum in terms of the upper and lower frequency compared to the CWT.



**Figure 6.** DWT energy distribution of different bearing faults (a) healthy (b) inner race (c) outer race (d) rolling elements; frequency spectrum for (e) healthy (f) inner race fault (g) outer race fault (h) rolling elements fault

Inner race fault was showed to be always diagnosable in envelope analysis regardless of which type of filter was used. A close look at the energy distribution of the decomposed signals in Figure 6, it was found that it has overall higher distributed energy in different frequency bands. Selecting the higher energy distribution frequency band in the wavelet based de-noising is just like the CWT de-noising. However, DWT decomposes the signal into resonance frequency bands with higher energy in the entire signal and quantify the energy content in the signal component.

Prior to envelope analysis, the SNR of both raw signal and wavelet de-noised signals were examined. The SNR has improved at least 2.5 dB after pre-processed using DWT. It was found that the 'db4' mother wavelet function with signal reconstruction reduce lesser noise compare to the CWT Morlet function. On other hand, the width of the resonance frequency would affect the overall pattern of the frequency spectrum. In this study, the resonance frequency band retained by the DWT is found to be different from the one in CWT. CWT have a cleaner spectrum compared to the DWT pre-processed opposite signal, however, some frequency components may lost and hence, other faults information also may be missed, because CWT filters eliminate the other frequency components and remain only resonant frequencies in the entire signal. Unlike, DWT which retained a wider frequency band due to the different wavelet function used which yield in wider fault's coverage. In this instance, the resonance frequency retained by DWT found to be contained the information of the misalignment and looseness as shown in Figure 6. The harmonic of the unit speed labeled by 1x, 2x and 3x indicated the looseness. Other than that, the 'db4' function in DWT produced similar pattern to the bearing impulse, however, when compared to the Morlet function in CWT, a distinct difference was found between them in the terms of the time and amplitude which resulted in differences in the frequency spectrum in terms of the upper and lower frequencies.

Moreover, it is also observed that the amplitude of the envelope spectrum for both bases are not the same. Signals pre-processed by DWT yielded more logical amplitude for the frequency spectrum in which the amplitude for BPFO was lower than BPFI. This fulfilled the theory that the vibration energy produced by outer race fault transmitted in a shorter distance to reach the sensor. Thus, the BPFO should have greater amplitude than BPFI.

**Table 2.** The summary of the amplitude of characteristic frequency for increased fault size.

Component	Fault Sizes	Characteristic frequency on spectrum				Frequency Spectrum Pattern
		CWT	Amplitude	DWT	Amplitude	
Inner race	0.007"	Prominent Peak	0.03686	Prominent Peak	0.0157800	Similar
	0.014"	Evidenced Peak	0.05390	Evidenced Peak	0.0390700	Similar
	0.021"	Evidenced Peak	0.34890	Evidenced Peak	0.1361000	Similar
Outer race	0.007"	Prominent Peak	0.01661	Prominent Peak	0.0310700	Similar
	0.021"	Evidenced Peak	0.02377	Evidenced Peak	0.0251900	Not Similar
	0.021" Orthogonal	Evidenced Peak	0.33230	Evidenced Peak	0.0527900	Not Similar

## 6. Conclusion

This paper presented the use of CWT and DWT and envelope analysis for resonance band demodulation. The CWT and DWT have proven to be an excellent filtering technique and resonant band demodulation methods to remove the unwanted frequency components from the signals. The proposed technique has shown to easier, faster and accurate to centre the band-pass filter for envelope analysis. The characteristic frequencies are evident in the frequency spectrum. Both CWT and DWT produced similar frequency spectrum pattern but different amplitude values, the distinguish similarity was the prominent characteristic frequency amplitude in the frequency spectrum. However, DWT has shown to be more superior as it is easier, less computational time, less noise and retained a wider frequency band which contained more faults diagnostic information. The frequency spectrum of rolling elements fault, found to be contained the characteristic frequency of inner race, outer fault and rolling element fault. It is also observed that the amplitudes of the characteristic frequencies increased when the fault occur and when the fault size increased. This feature could be used to distinguish the different bearing fault types, identify the fault locations and also assess the fault severities.

## 7. References

- [1] El-Thalji I and Jantunen E. 2015. A summary of fault modelling and predictive health monitoring of rolling element bearings. *Mechanical systems and signal processing*.**60**. 252-72
- [2] Yadav M and Wadhvani S. 2011. Automatic fault classification of rolling element bearing using wavelet packet decomposition and artificial neural network. *International Journal of engineering and technology*.**3**. 270-6
- [3] Samanta B and Al-Balushi K. 2003. Artificial neural network based fault diagnostics of rolling element bearings using time-domain features. *Mechanical systems and signal processing*.**17**. 317-28
- [4] Ak Chandel R P. 2013. Bearing Fault Classification Based on Wavelet Transform and Artificial Neural Network. *IETE Journal of Reseach*.**59**. 219-25
- [5] Bhavaraju K M, Kankar P, Sharma S C and Harsha S. 2010. A comparative study on bearings faults classification by artificial neural networks and self-organizing maps using wavelets. *International Journal of Engineering Science and Technology*.**2**. 1001-8
- [6] Yan W, Qiu H and Iyer N. 2008 Feature extraction for bearing prognostics and health management (phm)-a survey (preprint). ed Secondary. Yan W, Qiu H and Iyer N: DTIC Document)
- [7] Stalin S. 2014. Fault Diagnosis and Automatic Classification of Roller Bearings Using Time-Domain Features and Artificial Neural Network. *International Journal of Science and Research (IJSR)*.**3**. 824-51
- [8] Patel V. 2014. Recent Advanced In AI Based Intelligent Fault Techniques for Rolling Element Bearing—A Review.
- [9] Oulmane A, Lakis A and Mureithi N. 2014. Application of Fourier Descriptors & Artificial Neural Network to Bearing Vibration Signals for Fault Detection & Classification. *Universal Journal of Aeronautical & Aerospace Science*.**2**. 37-54
- [10] Gligorijevic J, Gajic D, Brkovic A, Savic-Gajic I, Georgieva O and Di Gennaro S. 2016. Online Condition Monitoring of Bearings to Support Total Productive Maintenance in the Packaging Materials Industry. *Sensors*.**16**. 316
- [11] Feng Z, Liang M and Chu F. 2013. Recent advances in time–frequency analysis methods for machinery fault diagnosis: a review with application examples. *Mechanical systems and signal processing*.**38**. 165-205
- [12] Yiakopoulos C and Antoniadis I. 2002. Wavelet based demodulation of vibration signals generated by defects in rolling element bearings. *Shock and Vibration*.**9**. 293-306
- [13] Yao D, Jia L, Qin Y and Yang J. 2014. Faults diagnosis of railway rolling bearing by using time-frequency feature parameters and genetic algorithm neural network. *Pulse*.**10**. 4
- [14] Rai A and Upadhyay S. 2016. A review on signal processing techniques utilized in the fault diagnosis of rolling element bearings. *Tribology International*.**96**. 289-306
- [15] Abdelrhman A M, Leong M S, Hee L M and Al-Obaidi S M A. 2015 *Book. Segregation of Close Frequency Components Based on Reassigned Wavelet Analysis for Machinery Fault Diagnosis: Springer*). pp.581-90
- [16] Abdelrhman A M, Leong M S, Hee L M and Ngui W K. 2015 A Comparative Study of Reassigned Conventional Wavelet Transform for Machinery Faults Detection. In: *Applied Mechanics and Materials*, pp. 90-4
- [17] Abdelrhman A M, Leong M S, Hee L M and Ngui W K. 2013 Application of wavelet analysis in blade faults diagnosis for multi-stages rotor system. In: *Applied Mechanics and Materials*. pp. 959-64
- [18] Jayakumar K and Thangavel S. 2015. Industrial drive fault diagnosis through vibration analysis using wavelet transform. *Journal of Vibration and Control*. 1077546315606602
- [19] Taylor J I and Vibration Consultants I. 1994. *The vibration analysis handbook*. (Vibration Consultants)
- [20] Jawadekar A, Paraskar S, Jadhav S and Dhole G. 2014. Artificial neural network-based induction motor fault classifier using continuous wavelet transform. *Systems Science & Control Engineering: An Open Access Journal*.**2**. 684-90

- [21] Vishwash B, Pai P S, Sriram N, Ahmed R, Kumar H and Vijay G. 2014. Multiscale slope feature extraction for gear and bearing fault diagnosis using wavelet transform. *Procedia Materials Science*.**5**. 1650-9
- [22] Feng G-J, Gu J, Zhen D, Aliwan M, Gu F-S and Ball A D. 2015. Implementation of envelope analysis on a wireless condition monitoring system for bearing fault diagnosis. *International Journal of Automation and Computing*.**12**. 14-24
- [23] Univesity C W R. 2016 Bearing Data Center. ed Secondary. Univesity C W R (United State: Case Western Reverse Univesity)